

Exploring the Biosynthesis of Metal Nanoparticles from *Coleus anthonyi* Leaf Extract: A Comprehensive GC-MS Analysis of a Novel Plant's Potential

Rosni Sunil¹, Jebin Joseph²  and T Sajini^{3*} ¹ Department of Chemistry, Bishop Kurialacherry College, Mahatma Gandhi University, Kottayam, India² Department of Botany, St. Berchmans College (Autonomous) Campus, Mahatma Gandhi University, Kottayam, India³ Department of Chemistry, St. Berchmans College (Autonomous) Campus, Mahatma Gandhi University, Kottayam, India

ABSTRACT

The development of plant extract-based and other green synthesis methods for fabricating nanomaterials has garnered significant attention due to their eco-friendliness and cost-effectiveness. This research focuses on the green synthesis, characterization, and dye degradation properties of silver nanoparticles (AgNP-CA) using the leaf extract of *Coleus anthonyi* (CA) and microwave irradiation. The synthesized nanoparticles were characterized using UV-visible spectrophotometry, X-ray diffraction, Fourier-transform infrared spectroscopy (FT-IR), dynamic light scattering (DLS), zeta potential analysis, and scanning electron microscopy. These characterizations confirm the successful synthesis of AgNP-CA from the leaf extract of *Coleus anthonyi*. Moreover, the observed monodisperse nanoparticle formation, with a size of 56.6 nm through DLS analysis, underscores the achievement of uniform particle size distribution. The recorded zeta potential value of -33.4 mV indicates the potential stability of the produced AgNP-CA. The synthesized AgNP-CA exhibited enhanced catalytic efficiency for degrading the organic dye, methyl orange, resulting in a significant reduction in its concentration. Furthermore, this study explores the major phytochemical content of *Coleus anthonyi* leaf extract using GC-MS analysis, revealing the presence of β -asarone, 9-(2-hydroxy-3-methyl-3-butenyl oxy)-4-methoxy furo(3,2-g)chromen-7-one, 1-phospha cyclopentadiene, 2,3,4,5-tetraethyl-1-oxo-1-phenyl, and 1,1'-biphenyl, 4-ethyl-4'-(4-propylcyclohexane). This comprehensive investigation highlights the potential of *Coleus anthonyi* leaf extract for the green synthesis of silver nanoparticles and underscores their promising catalytic applications.

KEYWORDS

Coleus anthonyi; GC-MS analysis; Green synthesis; Silver nanoparticle; Catalysis

Received: 17 September 2023, revised: 31 March 2024, accepted: 14 April 2024

INTRODUCTION

Nanotechnology has become one of the most rapidly growing fields of science and technology in recent years.^{1,2} With the emergence of nanotechnology, new possibilities have opened up in many areas, including electronics, energy, medicine, and materials science.^{3,4} The potential applications of nanotechnology are vast, and it is expected to revolutionize the world in the coming years. One of the critical aspects of nanotechnology is the synthesis and fabrication of nanomaterials with desired properties. Various methods, both physical and chemical methods, are employed for the synthesis of nanoparticles.⁵ The increasing emphasis on green chemistry and biological methods which are non-toxic, rapid, and cost effective have aroused much interest because of their simplicity and versatility.⁶⁻⁸ The development of green synthesis methods for the fabrication of nanomaterials has become a significant area of research due to its eco-friendliness and cost-effectiveness.⁹⁻¹¹ In this study, we have explored the green synthesis of silver nanoparticles using leaf extract of *Coleus anthonyi*, a newly discovered plant in the southwestern ghats region of India.

Coleus anthonyi (CA), a plant species belonging to the family Lamiaceae, was recently discovered in the southwestern ghats region of India by Jebin Joseph et al.¹² The plant has not been widely studied, and its potential applications in various fields remain largely unexplored. However, it is known that the plant contains various phytochemicals, including polyphenols, flavonoids, and terpenoids, which have been reported to have antioxidant, antimicrobial, and anticancer properties.^{13,14}

Several reports are available on the biological synthesis of metal nanoparticles such as silver and gold using plant extract as both reducing and stabilizing agents.^{15,16} Bacteria, yeast and fungi can also be

used for synthesizing nanoparticles.¹⁷ Green synthesis of nanoparticles using plant extracts has gained significant attention in recent years due to its eco-friendliness, cost-effectiveness, and ability to produce nanoparticles at a large scale.^{6,18} Several recent studies have investigated various plant extracts for their potential in synthesizing AgNPs using green chemistry approaches.¹⁹ While each study has its unique findings and contributions, we aim to provide a comparative analysis focusing on key aspects such as synthesis efficiency, nanoparticle morphology, stability, and potential applications.

The use of plant extracts for the synthesis of nanoparticles offers several advantages over traditional chemical methods, including the absence of toxic chemicals and the ability to produce nanoparticles at a large scale.²⁰ The reducing agents, such as polyphenols, flavonoids, and terpenoids, abundant in plant extracts, facilitate the reduction of metal ions to nanoparticles.¹³ Moreover, natural stabilizers like proteins, polysaccharides, and organic acids, inherent to these extracts, prevent the aggregation of nanoparticles, ensuring their sustained dispersion and stability.²¹ Microwave assisted synthesis using plant extract as both reducing and capping agent is a feasible approach for the rapid green synthesis of metal nanoparticles.^{22,23} Microwave irradiation offers rapid and uniform heating of the reaction medium and thus provides homogeneous nucleation and growth conditions for nanoparticles.^{24,25}

The use of AgNPs in various fields, including medicine, electronics, and environmental remediation, has been widely reported.²⁶⁻²⁸ AgNPs have excellent antimicrobial properties and have been used in the development of antimicrobial agents for various applications.^{7,15,29} AgNPs have also been reported to have anticancer properties and have been explored for the development of anticancer agents.^{30,31} In addition, AgNPs have been used in the development of sensors and electronic devices due to their unique electrical and optical properties.^{8,21} The green synthesis of AgNPs using plant extracts offers a more sustainable and eco-friendly alternative to traditional chemical methods.³²

*To whom correspondence should be addressed
Email: sajinijebin@sbccollege.ac.in

The main objective of this study is to explore the potential of *Coleus anthonyi* leaf extract for green synthesis of AgNPs and to investigate their potential applications in catalytic study. Gas chromatography-mass spectrometry (GC-MS) analysis will be carried out to identify the phytochemicals present in the leaf extract, which are responsible for the reduction of silver ions to AgNPs. The synthesized nanoparticles will be characterized using various techniques, including UV-Vis. spectroscopy, X-ray diffraction, and scanning electron microscopy. The microwave assisted method for the synthesis of AgNPs using the leaf extract of the plant is employed in the work. Along with green synthesis the catalytic activity of AgNPs is also investigated. The present study does not involve any toxic or harmful chemicals.

MATERIALS AND METHODS

Materials

Silver nitrate and ethanol were obtained from Merck, India. All the chemicals utilized were in their analytical grade form and were employed as acquired, without any additional purification process. All the aqueous solutions were prepared using distilled water.

Plant description and extraction methods

The leaves of *Coleus anthonyi* were used for phytochemical investigation and for AgNPs synthesis. *Coleus anthonyi* is a new species of plant belonging to the family Lamiaceae found in the southwestern ghats of India recently (Figure 1). This genus consists of annual or perennial herbs or shrubs and can be recognized by its 5 lobed calyx (1 upper, 4 lower) with pedicel attached asymmetrically to the base of calyx tube, opposite the posterior lip and usually, corolla with upper lip shorter than lower.¹²

The plant *Coleus anthonyi* was collected from Neyyar Dam, Thiruvananthapuram, India. The fresh plant collected was taxonomically identified and washed thoroughly with distilled water. The leaves were then separated and sliced into small pieces before being dried in a hot air oven. Subsequently, 20 g of the dried sample was taken in a round-bottom flask along with 150 mL of distilled water. The flask was fitted with a condenser and boiled for about 20 minutes. After boiling, the mixture was allowed to cool and then filtered through Whatman filter paper. The resulting extract was then stored in a refrigerator for further use. For phytochemical analysis, the air-dried leaves were crushed into powder form. About 15g of powdered specimen transferred into the extractor for sequential extraction using ethanol (250 mL) as a solvent for 48 hours. Filtered the mixture using filter paper to remove solid plant debris. Concentrated the filtrate



Figure 1: Image of *Coleus anthonyi*

using a rotary evaporator to remove the ethanol solvent and obtain a concentrated extract. Then dissolved the concentrated extract in a suitable solvent for GC-MS analysis, such as methanol. Evaporated the solvent under gentle conditions to obtain a residue of the purified ethanolic leaf extract. The purified extract further subjected to gas chromatography-mass spectrometry analysis. This purification procedure effectively removes impurities and concentrates the target compounds present in the ethanolic leaf extract, making it suitable for GC-MS analysis.³³

Synthesis of silver nanoparticles

90 mL of 1 mM silver nitrate solution was taken in a 250 mL beaker. To this about 10 mL of leaf extract was added and stirred well. The solution was then placed in a microwave oven and irradiated. The solution is collected after each 30 seconds and stored. The process is repeated for 4 minutes. The experiment is repeated for different leaf extract composition (5 mL, 15 mL). The obtained silver nanoparticles designated as AgNP-CA.

Characterization of leaf extract and AgNP-CA

The FT-IR spectra of the leaf extract and the synthesized AgNPs were analyzed and scanned. The data has been collected with resolution and wavenumber around 500-3500 cm^{-1} . FT-IR spectra of synthesized AgNP-CA were analyzed using Perkin Elmer-400 spectrometer with ATR attachment. The characterization of the AgNP-CA was analyzed using a UV-vis. spectrophotometer. The sample solution was diluted with distilled water and loaded in a cuvette. The spectral data obtained is in the range 300-700 nm. The analysis was carried out on Agilent Technologies Carry 5000 UV-vis. absorption spectrophotometer possessing a scanning speed of 2000 nm/min.

The dynamic scattering analysis (DLS) provides the idea about synthesized nanoparticles with respect to their size while zeta potential is used to know surface charge variation and colloidal stability of the nanoparticles. These studies were performed with nanoparticle analyzer HORIBA SZ-100. SEM-EDX gives a high-resolution image of the silver nanoparticle synthesized. This technique was used to identify the shape and size of the AgNP-CA. EDX gives information about the weight percentage of the silver. Images of the sample have been recorded. The study was performed with Carl Zeiss EVO 18 Research.

The XRD analysis is used to determine the lattice structure of the synthesized silver nanoparticle. For the X-ray diffraction studies of the composites Rigaku miniflex 600 XRD was utilized. GC-MS have been used to determine the trace constituents in the leaf extract CA. The technique combines the features of gas chromatography and mass spectrometry. The instrument used is Shimadzu Corporation, Japan Model: GCMS QP2010S.

In the gas chromatography-mass spectrometry (GC-MS) analysis, a column oven temperature of 70.0°C was maintained to facilitate the separation of compounds. Samples were injected at a high temperature of 260.00°C using a split injection mode. The flow control was set to linear velocity mode, with a pressure of 61.5 kPa and a total flow rate of 24.0 mL/min, wherein the column flow was maintained at 1.00 mL/min. This configuration ensured a linear velocity of 36.7 cm/sec for optimal separation efficiency. A purge flow of 3.0 mL/min and a split ratio of 20.0 were employed to enhance the chromatographic resolution. The ion source temperature was set to 200.00°C, while the interface temperature was maintained at 280.00°C to facilitate efficient ionization and transfer of analytes to the mass spectrometer. Solvent cut time of 6.50 min was implemented to ensure the removal of solvent peaks before analyte elution. The detector gain was set to relative mode with a gain of 1.06 kV, along with a threshold of 1000 for sensitive detection of compounds. These meticulously controlled conditions provided an optimal environment for the accurate identification and quantification of compounds in the ethanolic extract of CA.

Identification of components in the ethanolic leaf extract of CA was achieved through the utilization of their retention indices, and the interpretation of mass spectra was conducted using the National Institute of Standards and Technology (NIST) database.^{33–35} The spectra of the unknown components obtained from the CA leaf extract were compared with the standard mass spectra of known components stored in the NIST library. This comparative analysis enabled the identification of the compounds present in the CA leaf extract by correlating their spectral features with those of known compounds in the database.

Optimization methods

To obtain knowledge about the role of the green approach and its importance, AgNPs were synthesized both in microwave irradiation and at room temperature. The synthesis of AgNPs at room temperature was done by mixing 10 mL of the leaf extract with 90 mL of 1mM silver nitrate solution. The mixture was kept at room temperature for about 4 hours for the synthesis of nanoparticles. The analysis of formation of AgNP-CA was done by UV-vis. spectroscopy at periodic intervals (1 hour)

The effect of leaf extract on the synthesis was examined by changing the composition of the leaf extract (5 mL, 15 mL) and mixing them with 90 mL of 1 mM silver nitrate solution. The mixture was subjected to microwave irradiation for the synthesis of corresponding AgNPs. The role of concentration of silver nitrate solution in the synthesis of AgNPs was also observed by preparing 2 mM and 3 mM of AgNO₃ solution. The solution was mixed with 10 mL of leaf extract and subjected to microwave irradiation.

Catalytic activity study of AgNP-CA

The catalytic activity of synthesized AgNP-CA was examined by observing the reduction of organic dye, methyl orange, by sodium borohydride. In a quartz cell about 0.5 mL (0.06M) NaBH₄ solution, 2 mL 0.1 mM methyl orange and 0.5 mL AgNP-CA solution were mixed. Using UV-vis. spectrophotometry the change in concentration of methyl orange with time was studied. The reduction of dye catalyzed by AgNPs was monitored in 10 min intervals and the absorption spectra were recorded in the range 340-800 nm.

RESULTS AND DISCUSSION

Characterization of CA leaf extract

GC-MS analysis

Gas chromatography-mass spectrometry (GC-MS) is a powerful analytical technique widely used for the identification and characterization of bioactive compounds present in various samples, including leaf extracts. GC-MS combines the principles of gas chromatography (GC) and mass spectrometry (MS) to separate, detect, and analyze complex mixtures of compounds. By comparing the observed data (retention time, peak area, peak height, and mass spectral fragmentation patterns) for each peak with the known data stored in the National Institute of Standards and Technology (NIST) database, it is possible to identify the compounds present in the ethanolic leaf extract of CA.

Identification of bioactive compounds: The GC-MS analysis of the ethanolic leaf extract of CA has revealed four major peaks (Figure 2) representing different bioactive compounds, namely β -asarone, 9-(2-hydroxy-3-methyl-3-butenyl oxy)-4-methoxy furo (3,2-g) chromen-7-one, 1-phospha cyclopentadiene, 2,3,4,5-tetraethyl-1-oxo-1-phenyl, and 1,1'-biphenyl, 4-ethyl-4'-(4-propylcyclohexane). These compounds were identified by correlating their peak retention time, peak area, and peak height with known compounds listed in the NIST database.

Validation of retention time and peak parameters: Table 1 provides details of the retention time, peak height, and peak area exhibited by the major bioactive compounds present in the CA leaf extract. These parameters are crucial for accurate compound identification and quantification. Validation involves comparing these values with known standards and ensuring consistency and reproducibility across multiple analyses.

Comparison of mass spectra: Figures 3 and 4 depict the mass spectra of the identified compounds obtained from the CA leaf extract and the corresponding spectra from the NIST library, respectively. The mass spectra provide information about the molecular structure and fragmentation pattern of each compound. Validation involves

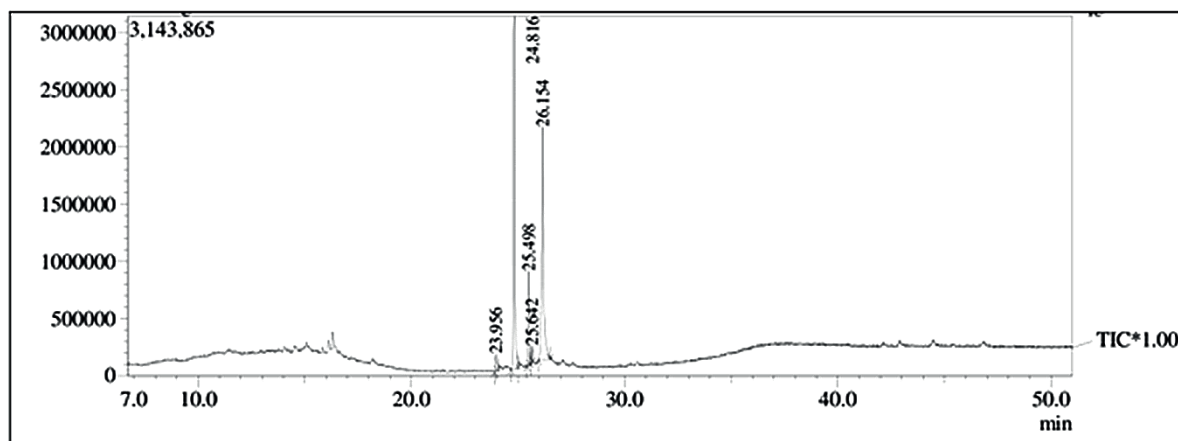


Figure 2: Gas chromatogram of ethanolic CA leaf extract

Table 1: Bioactive compounds found in ethanolic extract of CA

Retention Time (min)	Peak Area (%)	Peak Height (%)	Compound Name
23.956	2.67	2.40	β -asarone
24.816	42.94	49.47	9-(2-hydroxy-3-methyl-3-butenyl oxy)-4-methoxy furo(3,2-g) chromen-7-one
25.498	10.10	13.23	1-phosphacyclopentadiene,2,3,4,5-tetraethyl-1-oxo-1-phenyl
26.154	42.87	32.63	1,1'-biphenyl,4-ethyl-4'-(4-propylcyclohexane)

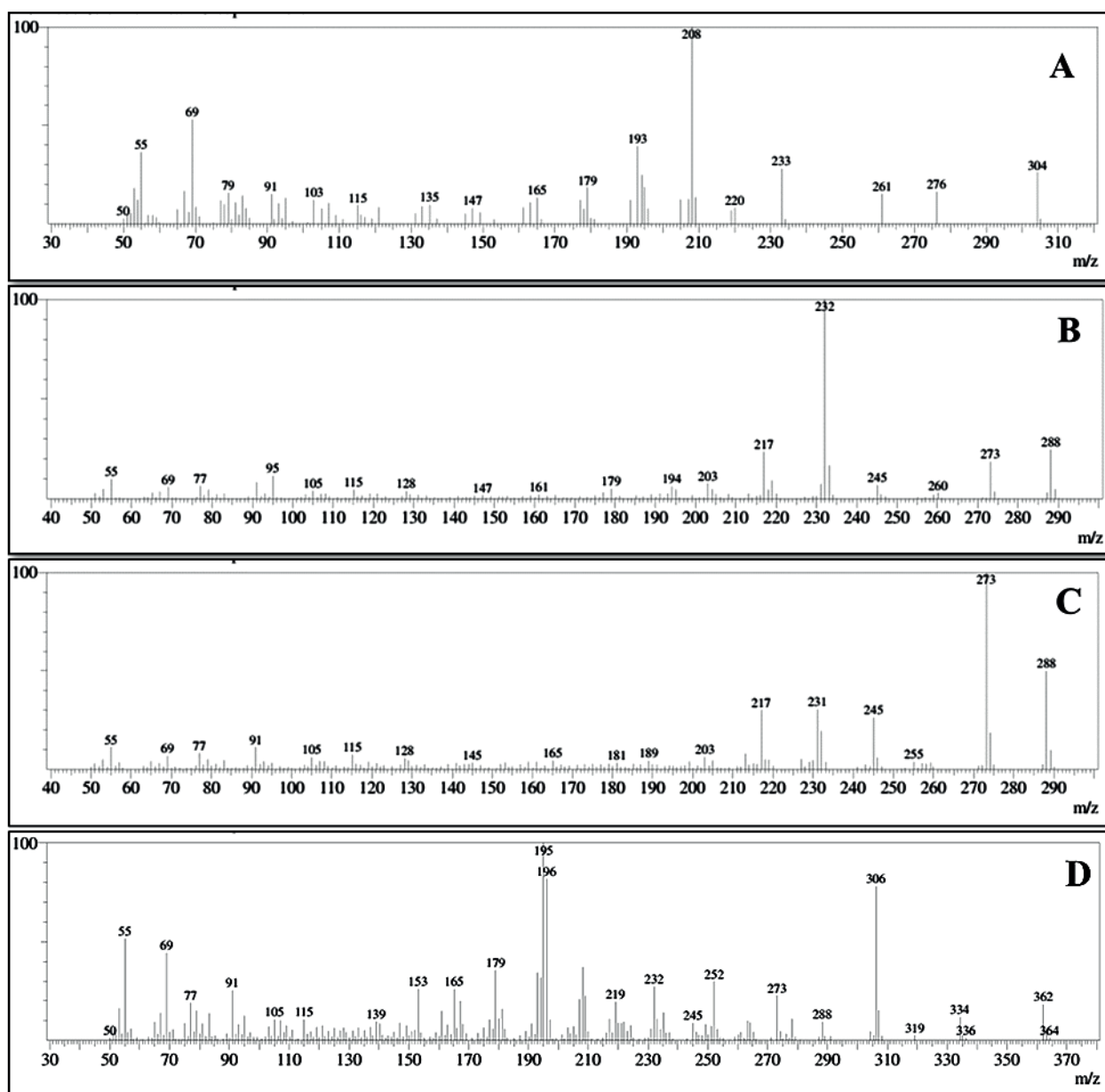


Figure 3: Mass spectrum of (A) β -asarone, (B) 9-(2-hydroxy-3-methyl-3-butenyl oxy)-4-methoxy furo(3,2-g)chromen-7-one, (C) 1-phospha cyclopentadiene,2,3,4,5-tetraethyl-1-oxo-1-phenyl and (D) 1,1'-biphenyl,4-ethyl-4'-(4-propylcyclohexane)

comparing the experimental mass spectra with the reference spectra in the NIST library to confirm the identity of the compounds.

Verification of peak assignment: Each peak in the chromatogram corresponds to a specific compound, and peak assignment is based on retention time, peak shape, and mass spectral characteristics. Validation involves verifying the accuracy of peak assignment by confirming that the retention time, peak shape, and mass spectral fragmentation pattern match those of known compounds in the NIST library.

Among the phytochemicals identified, β -asarone is referred to as carcinogenic by the council of Europe committee of experts on flavoring substances.³⁶ These compounds also exhibit anti-fungal properties by inhibiting ergosterol biosynthesis in *Aspergillus niger*.³⁷ Thus, due to the carcinogenic property of these compounds it is difficult to use them in medications.

Fourier transform - infrared spectroscopy

FT-IR results (Figure 5) confirm the presence of several functional groups in the ethanolic leaf extract of *Coleus anthonyi*, including hydroxyl groups, alkanes, aldehydes, amines, sulfones/sulfonyl, and

alcohols/ethers/esters/carboxylic acids/anhydrides. These functional groups are indicative of the presence of various organic compounds in the extract. The peak obtained at 3228 cm^{-1} confirms the presence of -OH functional group suggests the presence of alcohols or phenols in the extract. Peaks at 2918 cm^{-1} (alkanes), suggests the presence of hydrocarbons in the extract. The peaks at 2848 cm^{-1} (aldehyde), 1633 cm^{-1} (amines), 1363 cm^{-1} (sulfones, sulfates, sulfonamides) and 1240 cm^{-1} (alcohols, ether, ester, carboxylic acid, anhydrides), 1035 cm^{-1} (fluoride) revealed the presence of various functional group. These functional groups are indicative of the presence of various organic compounds in the extract.

Synthesis of AgNP-CA

Through the application of microwave radiation, the initial synthesis of AgNPs commenced by subjecting a mixture of 90 mL of 1 mM AgNO_3 solution and 10 mL of CA leaf extract to microwave irradiation. Notably, the combination of leaf extract and AgNO_3 solution yielded no discernible color alteration. The alteration in color observed during the analysis when exposed to microwave irradiation, serves as a valuable indicator for optimization (Figure 6). The progressive shift

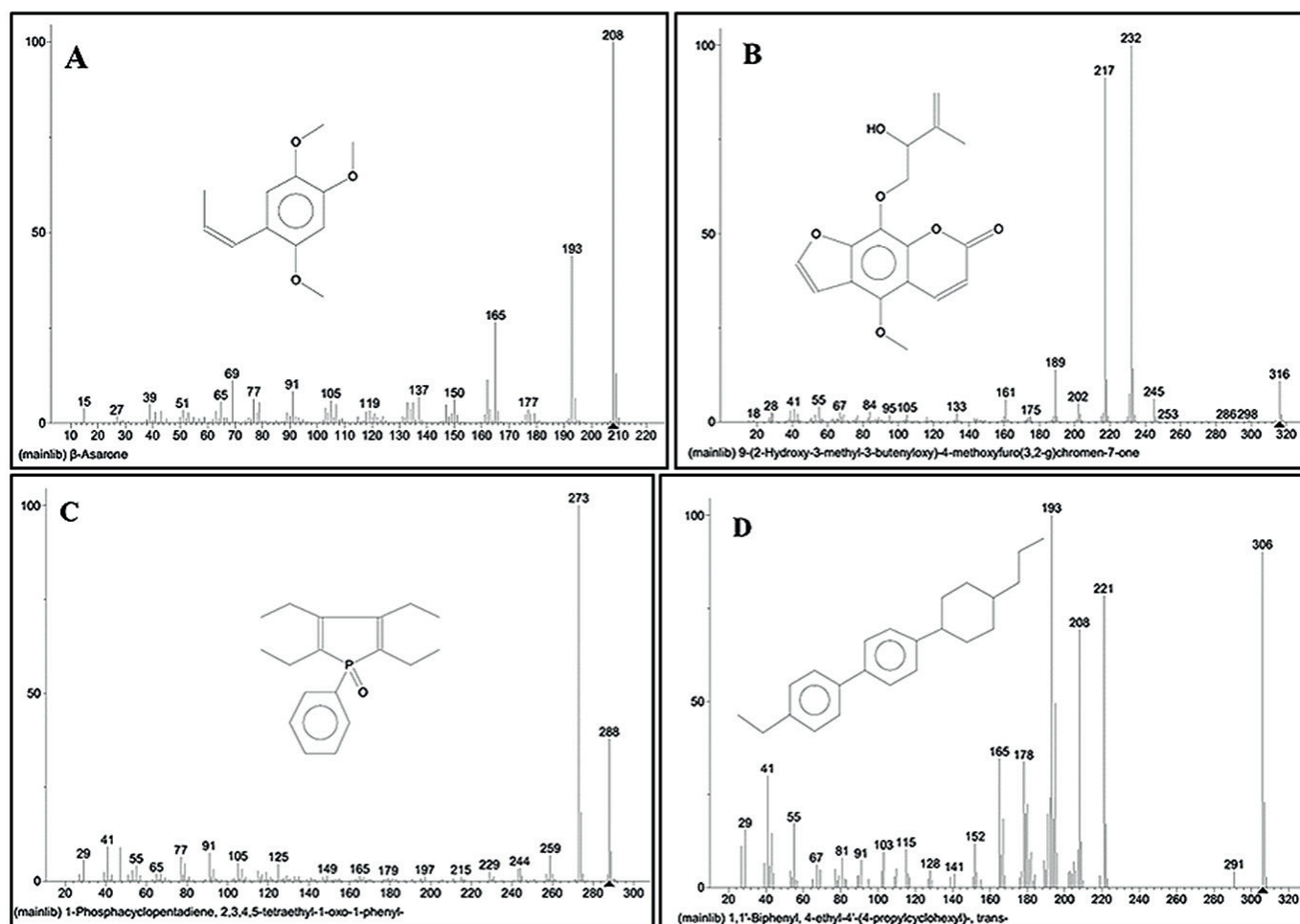


Figure 4: Mass spectrum obtained from NIST library (A) β -asarone, (B) 9-(2-hydroxy-3-methyl-3-butenyl oxy)-4-methoxy furo(3,2-g)chromen-7-one, (C) 1-phosphacyclopentadiene,2,3,4,5-tetraethyl-1-oxo-1-phenyl and (D) 1,1'-biphenyl,4-ethyl-4'-(4-propylcyclohexane)

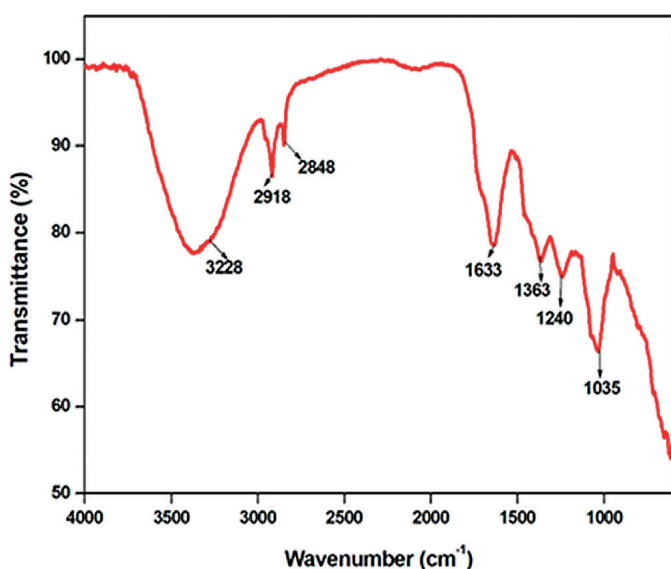


Figure 5: FT-IR spectrum of ethanolic leaf extract of CA

from an initially colorless appearance to a final yellowish-brown hue signifies the successful formation of AgNPs through the reduction of silver nitrate mediated by the leaf extract.¹⁹ The color changes observed during the formation of AgNPs are a consequence of the size-dependent surface plasmon resonance (SPR) effect and alteration of Ag^+ ions to Ag^0 by aqueous extracts.³⁸ When AgNPs are synthesized and begin to form, they exhibit unique optical properties due to the

interaction of light with the collective oscillations of conduction electrons on the nanoparticle surface. This leads to the absorption and scattering of specific wavelengths, resulting in the characteristic color shifts that are indicative of nanoparticle synthesis and growth.

Characterization of AgNP-CA

UV-visible spectrophotometry

The UV-vis. spectroscopy provides confirmation about the formation of AgNPs. The reaction medium shows absorption maxima in the range of 300-700 nm due to surface plasmon resonance of AgNPs.^{39,40} The reduction of silver nitrate by the leaf extract causes the formation of AgNPs. The color change observed was a primary confirmation on the formation of AgNPs. This can be further confirmed using UV-vis. spectroscopy analysis. Figure 7 shows the UV-vis. spectra of AgNPs synthesized using the leaf extract of CA by 4 min of microwave irradiation. The presence of an absorption band within the wavelength range of 400-500 nm in the spectrum can be attributed to a phenomenon known as surface plasmon resonance (SPR).^{41,42} This absorption band indicates the interaction of light with the collective oscillation of conduction electrons on the surface of the AgNPs synthesized using the CA extract.

The increase in peak intensity over time, with a pronounced peak at 4 minutes, signifies a progressive accumulation of silver nanoparticles in the solution. This suggests that the rate of AgNP-CA formation is relatively high, leading to a higher concentration of nanoparticles as the reaction proceeds. The significant peak intensity at 4 minutes further implies that this specific duration allows for the optimum synthesis of AgNPs, resulting in a substantial yield.

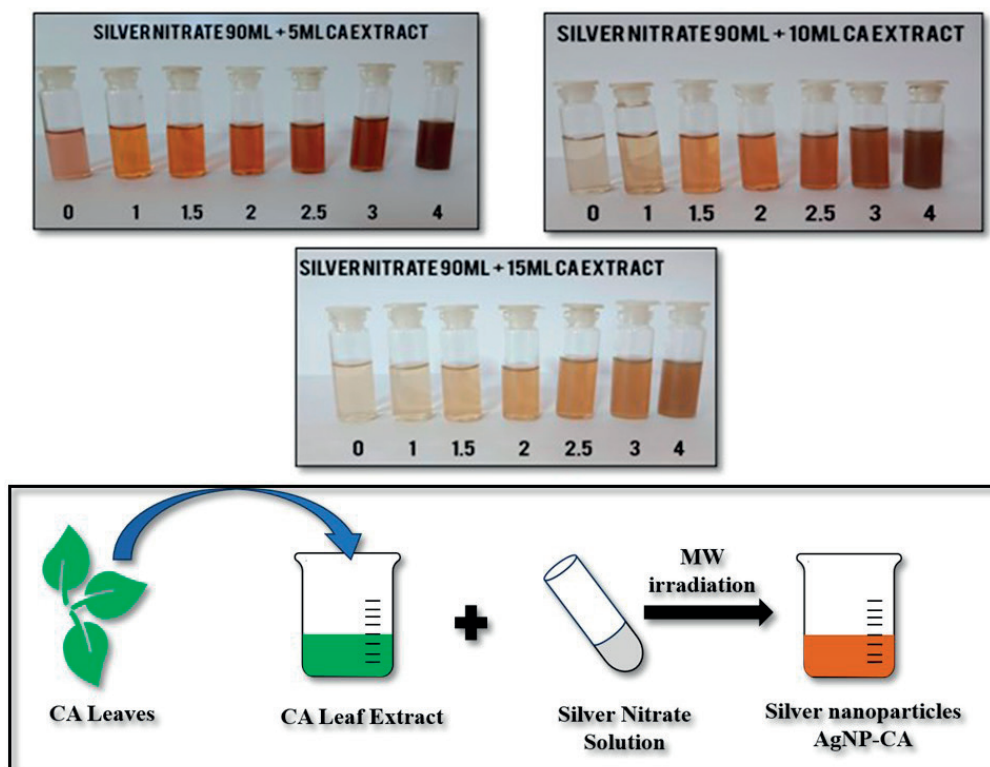


Figure 6: Evolution of color in different AgNP-CA solution during 30 second intervals of microwave irradiation and its schematic representation

The absorption peak's characteristics in the UV-vis. spectrum provide valuable insights into the role of the chemical constituents present in the CA extract. The chemical compounds within the extract act as reducing agents, playing a pivotal role in the reduction of silver ions (Ag^+) from the silver nitrate (AgNO_3) solution. These compounds facilitate the conversion of Ag^+ ions to AgNPs by providing electrons for the reduction reaction.

The mechanism involved in the formation of AgNP-CA depicted in Scheme 1 and described as follows. The synthesis of silver nanoparticles (AgNP-CA) using leaf extracts involves a straightforward yet intricate process. Initially, phytochemicals present in the leaf extract, such as polyphenols and flavonoids, act as reducing agents, donating electrons to silver ions (Ag^+) derived from a silver salt precursor.⁴³ This reduction leads to the formation of silver atoms (Ag^0) which then aggregate and nucleate, forming small clusters.⁴⁴ Further reduction and aggregation processes occur, facilitated by the continual supply of reducing agents from the leaf extract. As the clusters grow, phytochemicals in the extract adsorb onto the surface of the nanoparticles, stabilizing them and preventing their aggregation. This dual role of phytochemicals as reducing agents and stabilizing agents ensures the formation of well-dispersed and stable AgNPs.

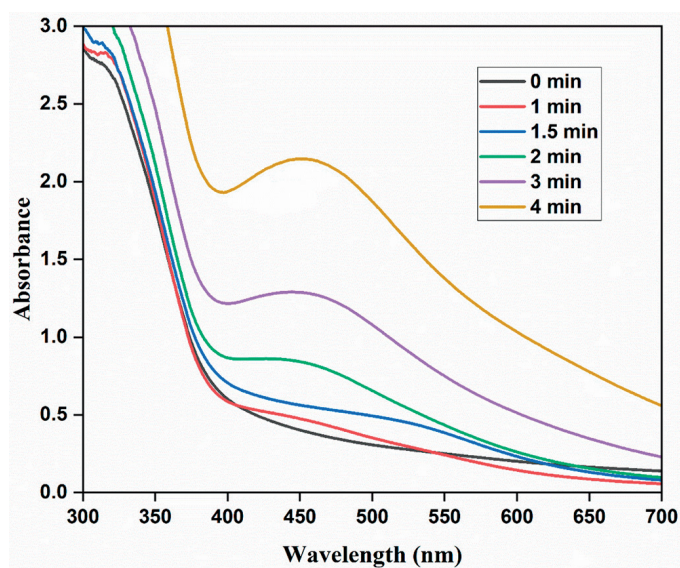
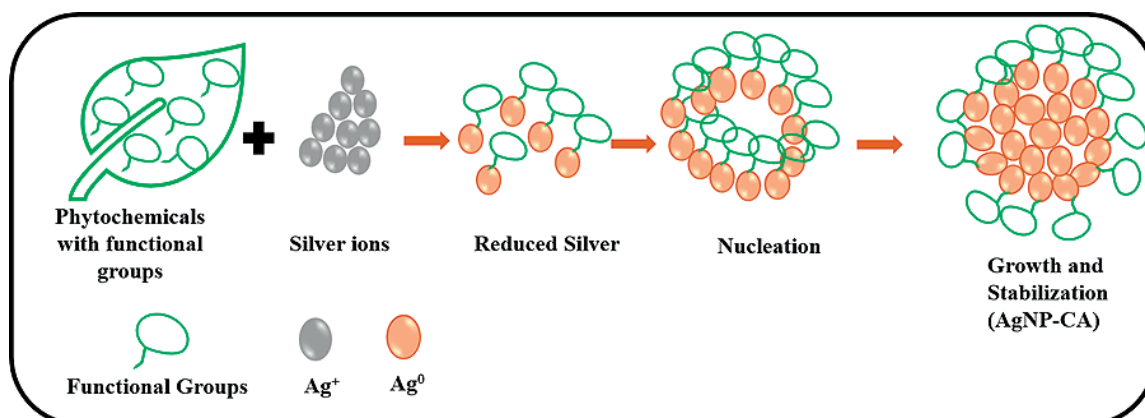


Figure 7: UV-vis. spectrum of AgNP-CA



Scheme 1: Schematic representation for the formation of AgNP-CA

The synthesis of silver nanoparticles at room temperature (27 °C) was also observed by UV-vis. spectra. Figure 8 shows the spectrum of silver nanoparticles synthesized at room temperature for about 4 hour.

The effect of temperature in the synthesis of AgNP can be understood from Figure 7 and 8. The disparity in the appearance of a characteristic AgNP peak in the UV-vis. spectrum between room temperature synthesis and microwave irradiation can be attributed to the distinct kinetics and thermodynamics of the two synthesis methods. Microwave irradiation offers several advantages, including rapid and efficient heating, which can lead to more favorable reaction conditions for nanoparticle formation.^{14,40} The higher temperatures achieved during microwave irradiation can enhance the reduction of silver ions, promote nucleation, and accelerate the growth of nanoparticles. This controlled and rapid process results in a more efficient formation of AgNPs with well-defined sizes, leading to the emergence of a SPR absorption peak in the UV-vis. spectrum. In contrast, room temperature synthesis might involve slower kinetics, potentially leading to the formation of smaller nanoparticles, weakly defined SPR peaks, or even incomplete nanoparticle formation, which can result in the absence of the characteristic Ag peak in the UV-vis. spectrum. The microwave-assisted synthesis provides a more conducive environment for achieving the necessary reaction rates and thermodynamic conditions that favor the production of silver nanoparticles with distinct optical properties, thus leading to the observed differences in the UV-vis. spectra.

Similarly, the influence of composition of CA leaf extract and concentration of silver nitrate in the synthesis of AgNPs can also be analyzed using UV-vis. spectroscopy. Figure 9 and Figure 10 shows the spectrum obtained in both the cases.

The provided data, depicted in Figure 9, illustrates the impact of varying concentrations (5 mL, 10 mL, and 15 mL) of CA leaf extract on the formation of AgNP-CA. Analysis of the spectral data reveals a discernible trend: as the quantity of CA extract decreases, there is an observable increase in the production of AgNP-CA. This suggests an inverse relationship between the amount of CA extract and the resulting AgNP-CA concentration. Particularly noteworthy is the outcome observed with 5 mL of CA extract, which corresponds to the highest peak intensity among the tested concentrations. This pronounced peak signifies a substantial concentration of AgNP-CA formed under these conditions.

The data presented in Figure 10 elucidates the impact of varying concentrations of silver nitrate (AgNO_3) solution on the resulting outcome. A closer examination of the spectrum reveals a clear and consistent pattern: as the concentration of AgNO_3 solution increases, there is a corresponding rise in absorbance values. This observed relationship between concentration and absorbance signifies a direct correlation, where higher concentrations of AgNO_3 lead to greater absorbance levels. This, in turn, implies a direct association between the concentration of AgNO_3 and the formation of AgNP-CA. Specifically, as the concentration of AgNO_3 solution increases, the production of AgNP-CA also increases, as indicated by the escalating absorbance values. In essence, the data underscores that higher concentrations of AgNO_3 solution result in a more pronounced formation of AgNP-CA, thereby highlighting the crucial role of AgNO_3 concentration in governing the synthesis process.

Fourier transform - infrared spectroscopy

The FT-IR spectroscopy is used to identify the biomolecules that cause the reduction of silver nitrate to silver as well as the functional groups present in the sample.^{45,46} Figure 11 depicts the FT-IR spectrum of AgNP-CA and aqueous leaf extract of CA. A broad band is obtained in the range $3400\text{--}3200\text{ cm}^{-1}$ due to --OH stretching indicating the presence of an alcoholic group in CA leaf extract.⁴⁷ The absorption peak at 2145 cm^{-1} typically corresponds to the stretching frequency of C=C bond in an alkyne functional group. The peak indicates the

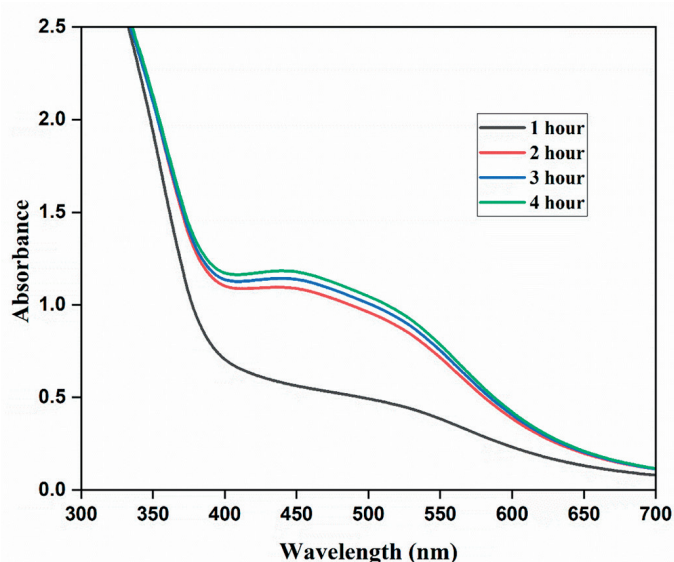


Figure 8: UV-vis. spectrum of AgNP-CA at room temperature

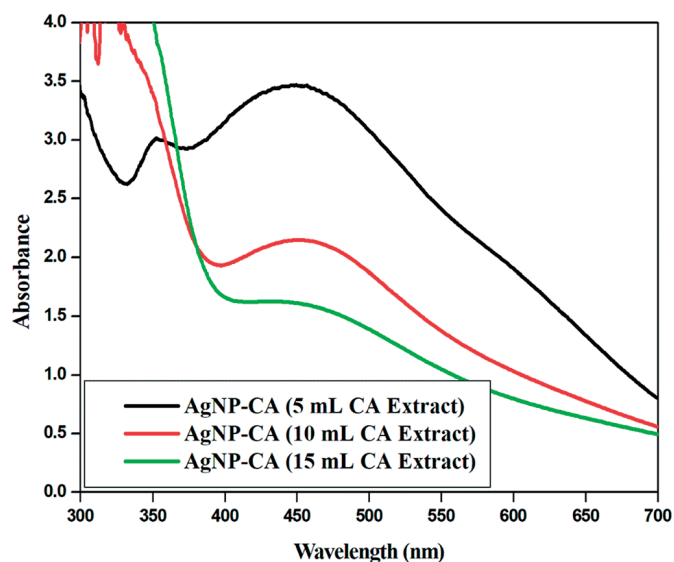


Figure 9: UV-vis. spectrum of AgNP-CA from 5-10 mL CA extract

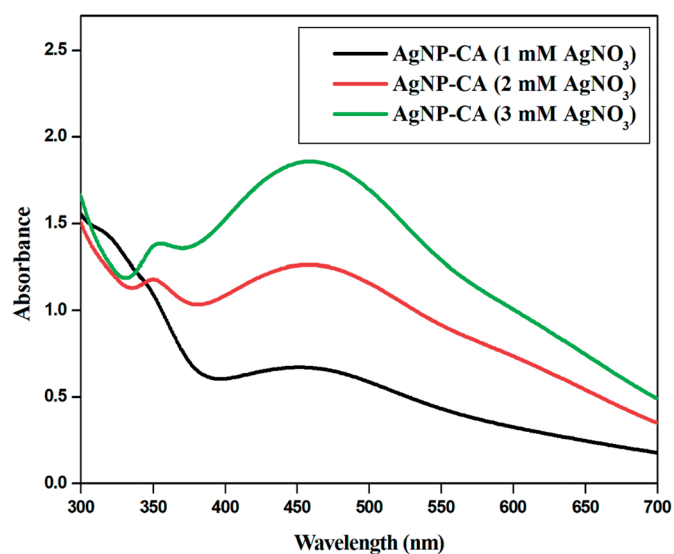


Figure 10: UV-vis. spectrum of AgNP from 1-3mM AgNO_3 solution and 10ml CA extract

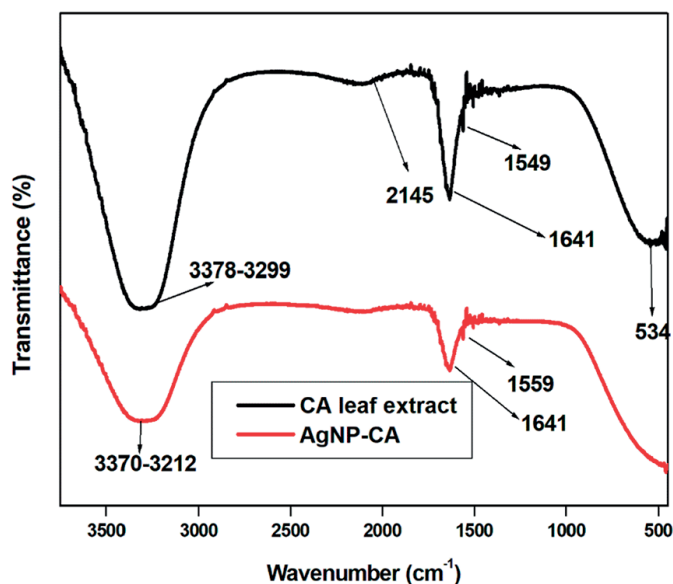


Figure 11: FT-IR spectrum of AgNP-CA and aqueous leaf extract of CA

presence of an alkyne group in the molecule being analyzed. It is noted that the exact stretching frequency can vary slightly depending on its chemical environment. However, in general the alkyne group has stretching in the range 2100–2260 cm^{-1} . The C=N stretching (imine/oxime) is indicated by the peak at 1641 cm^{-1} and N-O (nitro compound) stretching is indicated by the peaks at 1549 cm^{-1} respectively.⁴⁰

The characteristic -OH stretching of the AgNP-CA is represented by the broad spectrum in the range 3370–3212 cm^{-1} . The peak at 1641 cm^{-1} indicates C=N stretching similar to that of CA extract. The decrease in intensity is due to resonance. The FT-IR spectrum of both CA extract and AgNP-CA shows a decrease in wavenumber. The slight decrease is due to the reaction taking place between the leaf extract and silver nitrate. The reduction taking place is due to the different functional groups present in CA extract. The leaf extract and silver nanoparticle shows an equivalent peak due to C=N stretch.

Dynamic light scattering (DLS)

The hydrodynamic size of the silver nanoparticle synthesized from CA extract can be determined using DLS analysis (Figure 12). The determination of an average particle size of 56.6 nm through DLS analysis for AgNP-CA underscores the achievement of monodisperse nanoparticle formation.^{30,48} This outcome signifies that a substantial majority of the nanoparticles cluster around the 56.6 nm mark, reflecting a relatively uniform size distribution. Such monodispersity points to a well-controlled synthesis process, where conditions were optimized to facilitate consistent nucleation and growth mechanisms. The observed size uniformity can be attributed to stable and controlled reaction conditions, where factors like temperature, reactant concentrations, and reaction duration were carefully regulated. This monodisperse characteristic is indicative of a successful and controlled synthesis approach, aligning with the desired outcome of producing nanoparticles with a uniform size distribution.

Zeta potential analysis

The zeta potential value is a measure of the surface charge of the nanoparticles. The recorded zeta potential value (Figure 13) of -33.4 mV serves as an indicator of the potential stability of the produced AgNP-CA.⁴⁹ This negative zeta potential value signifies strong electrostatic repulsion forces among the nanoparticles, contributing to their long-term stability and effective dispersion within the solution.^{50,51} The substantial negative charge on the nanoparticle surfaces results in repulsive interactions, preventing agglomeration and ensuring a

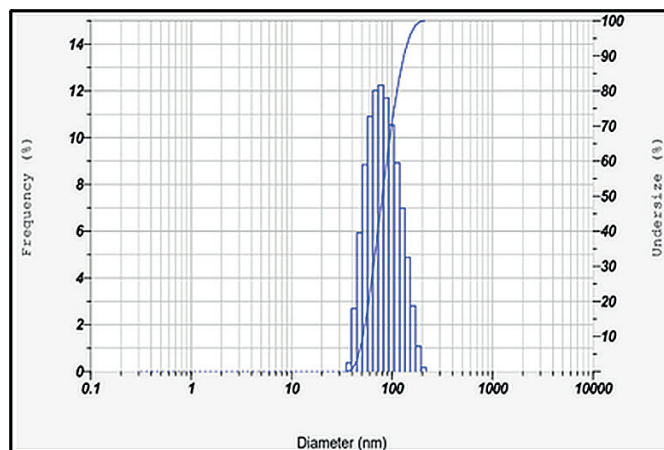


Figure 12: Graph showing the hydrodynamic size of AgNP-CA extract

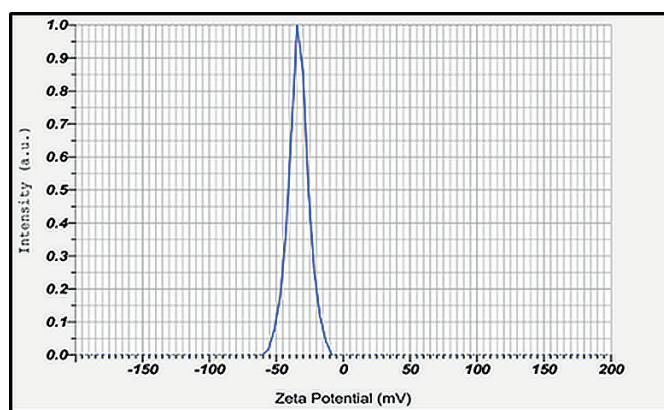


Figure 13: Graph showing the zeta potential analysis of AgNP-CA extract

good colloidal nature. The observed high dispersity, attributed to the negative-negative repulsion, further validates the successful synthesis and stabilization of the AgNP-CA, which enhances their suitability for various applications requiring sustained stability and even dispersion.

Scanning electron microscopy (SEM)

The SEM analysis was used to determine the shape and size of the synthesized silver nanoparticle. The confirmation of silver nanoparticle formation and their morphological characteristics as nearly spherical shapes through SEM analysis (Figure 14) underscores the influence of capping agents present in the CA leaf extract on the synthesis process.⁵¹ The spherical shape, which are found to be an aggregate, observed is likely attributed to the specific interactions between the capping agents and the growing nanoparticles.⁵² Capping agents are molecules from the leaf extract that can adsorb onto the nanoparticle surfaces during their formation, effectively guiding the growth process and influencing their final morphology. In this case, the availability and nature of these capping agents within the CA leaf extract contribute to the preference for spherical morphology. The controlled interaction between the capping agents and the nanoparticles ensures a uniform growth pattern, resulting in the distinctive spherical shape observed in the SEM analysis.

EDX analysis

The validation of elemental silver's presence was established through Energy Dispersive X-ray (EDX) analysis, evident by the detection of a characteristic signal at 3 keV (Figure 15). This outcome directly aligns with silver being a principal component within the synthesized nanoparticles. Furthermore, the EDX analysis also revealed the presence of other elements including C, O, Cl, Al, and N, with

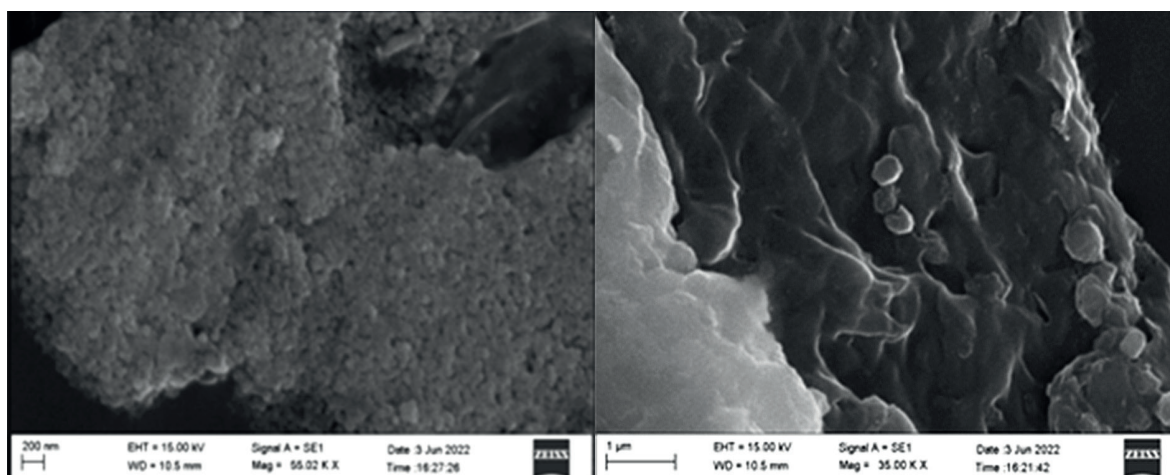


Figure 14: SEM images of AgNP-CA in different magnifications

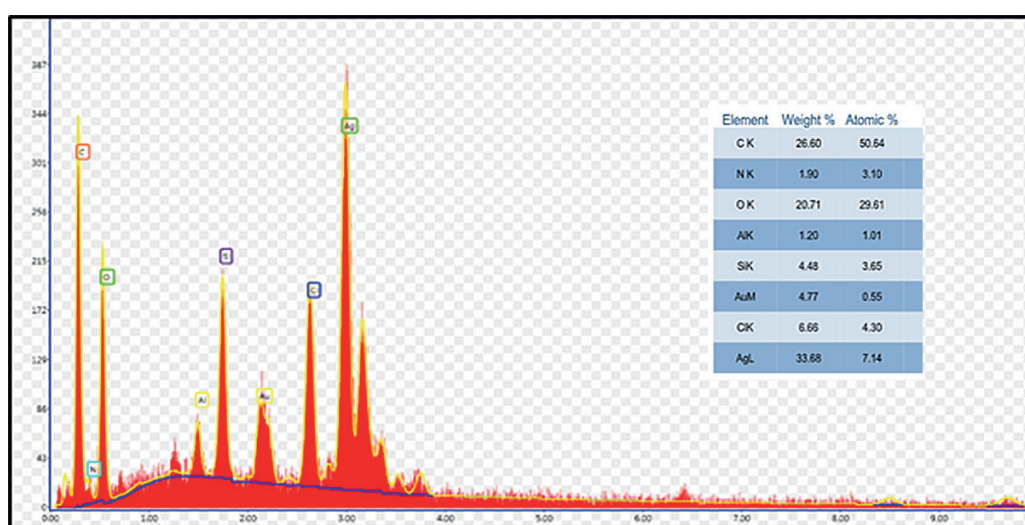


Figure 15: EDX spectrum of AgNP-CA

weaker signals.¹⁰ This diversity of elements can be attributed to the incorporation of phytochemicals and compounds associated with the CA leaf extract onto the surface of the AgNPs. The interaction of these phytochemicals with the nanoparticle surfaces is reflected in the EDX data and underlines the role of various elements from the leaf extract in contributing to the composition and potential properties of the resulting AgNPs.

X-ray diffraction

The X-ray diffraction technique gives an insight into the crystallographic nature of the synthesized silver nanoparticle.⁴⁷ The XRD analysis results, as shown in Figure 16, reveal distinct diffraction peaks occurring at angles 28.5°, 32.9°, 38.8°, 46.9°, 65.2°, and 78.0°. These peaks correspond to the crystallographic planes (100), (110), (111), (200), (220), and (311) of a face-centered cubic (FCC) structure for silver nanoparticles.⁹ This crystallographic arrangement is consistent with the data provided by the Joint Committee on Powder Diffraction Standards (JCPDS), with reference to file number 04-0783.^{11,51}

The relative intensity of these diffraction peaks offers insights into the orientation and arrangement of crystal planes within the nanoparticles. Notably, the intensity of the (111) plane diffraction peak appears particularly pronounced, indicating that this plane is preferentially oriented parallel to the direction of the incident X-ray light.⁵³ This suggests a strong alignment of the (111) planes in the sample, which can be attributed to the synthesis method employed and the crystalline growth mechanism of the nanoparticles.

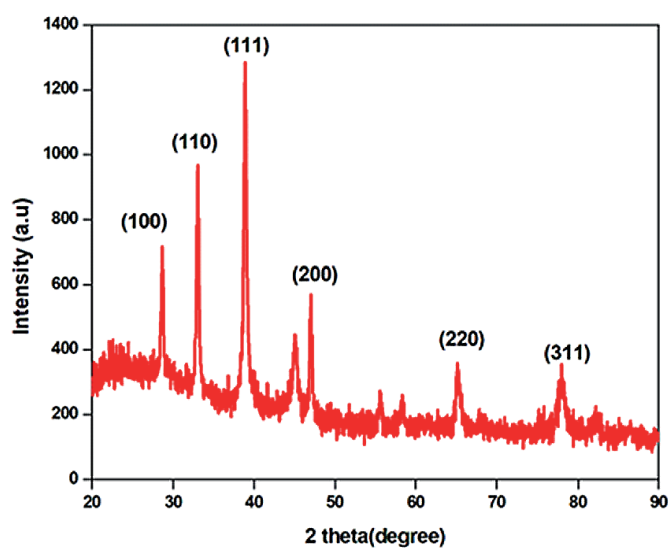


Figure 16: X-ray diffraction pattern of AgNP-CA

Catalytic reduction of methyl orange

The assessment of metal nanoparticles' catalytic potential typically involves the observation of organic dye reduction through the use of sodium borohydride (NaBH₄). Organic dyes exhibit distinct colors in both their oxidized and reduced states, and it is essential that

the surface plasmon resonance (SPR) band of metal nanoparticles does not interfere with the dye's absorption maximum. For the investigation of the catalytic properties of the synthesized AgNP-CA, azo dyes like methyl orange were chosen.⁵⁴ Methyl orange, in its aqueous form, appears orange-red, and upon reduction, it becomes colorless. The UV-visible spectrum displays an absorption maximum at 465 nm, a characteristic feature owing to the presence of azo groups within the dye.⁵⁵ Importantly, the SPR of silver nanoparticles is distinct from this wavelength.

In the absence of the silver nanocatalyst, the reduction of dyes by NaBH_4 proceeds at a notably sluggish pace, with peak intensity remaining unchanged for several hours. However, upon the addition of the catalyst, the color of methyl orange visibly faded within one hour. This change was accompanied by a noticeable alteration in peak intensity, as depicted in Figure 17. The presence of the nanocatalyst significantly enhances the reaction rate. The absorbance decreased in the presence of the nanocatalyst, confirming the reduction in methyl orange concentration. Remarkably, the reaction was completed within one hour in the presence of AgNP-CA, indicating its catalytic role in the reduction of azo dyes. In contrast, without the catalyst, it would take hours to observe any change in the UV-visible spectrum. Scheme 2 provides a schematic representation of the degradation process of methyl orange.

Comparative analysis

Our study demonstrates the efficient synthesis of silver nanoparticles (AgNPs) using CA leaf extract, showcasing a high yield of well-defined nanoparticles. Comparative studies have shown similar synthesis efficiencies for other plant extracts, including aloe vera, green tea, and neem leaf extracts, indicating the widespread applicability of plant-mediated synthesis methods.^{15,20}

The morphology of AgNPs synthesized using different plant extracts can vary significantly.⁵⁶ While our study reports the formation of predominantly spherical AgNPs with narrow size distribution, other

plant extracts have been shown to produce AgNPs with diverse shapes such as triangular, hexagonal, and rod-like structures. The choice of plant extract and synthesis conditions can influence nanoparticle morphology.¹⁵

The stability of AgNPs is crucial for their potential applications in various fields.⁵⁷ Our research highlights the excellent stability of AgNPs synthesized using *Coleus anthonyi* leaf extract, as evidenced by long-term colloidal stability and minimal aggregation. Comparative studies have reported similar findings, with AgNPs synthesized using various plant extracts exhibiting good stability under different environmental conditions.

AgNPs synthesized using plant extracts possess versatile properties that make them suitable for a wide range of applications, including antimicrobial, catalytic, and biomedical applications.^{26,58,59} Our study explores the potential of AgNPs synthesized from *Coleus anthonyi* leaf extract for biomedical applications, such as drug delivery and therapeutics. Comparative studies have demonstrated the effectiveness of AgNPs synthesized from different plant extracts in antimicrobial and catalytic applications, showcasing their potential in combating microbial infections and environmental pollutants.

CONCLUSION

The future of green synthesis strategy which uses economic and renewable sources while getting rid of the possible hazards is a huge step to advancement. The present research work focused on the synthesis and characterization of metal nanoparticles using *Coleus anthonyi* leaf extract, aiming to unveil the potential of this newly discovered plant through GC-MS analysis. The study successfully synthesized silver nanoparticles using the leaf extract of *Coleus anthonyi* as a reducing and stabilizing agent.

The GC-MS analysis of the ethanolic extract of *Coleus anthonyi* provided valuable insights into the phytochemical composition of the plant, highlighting the presence of various bioactive compounds. This analysis further confirmed the plant's potential for nanoparticle synthesis due to the abundance of natural reducing and capping agents. The phytochemical analysis of the new species *Coleus anthonyi* provides a better insight into the plant and can be utilized for further applications.

The synthesized AgNP-CA were comprehensively characterized using a range of techniques, including UV-vis. spectroscopy, X-ray diffraction, FT-IR, DLS, zeta potential analysis, and scanning electron microscopy. These analyses confirmed the successful formation of silver nanoparticles with distinct physicochemical properties. The catalytic efficiency of AgNP-CA was evaluated through the degradation of methyl orange, a common organic dye. The nanoparticles exhibited enhanced catalytic activity, indicating their potential applications in environmental remediation and wastewater treatment. The optimization studies revealed the significance of microwave irradiation and the amount of leaf extract in nanoparticle synthesis. Microwave conditions were found to be favorable for the synthesis process, providing a cost-effective and energy-efficient approach. Moreover, the leaf extract played a crucial role in the reduction and stabilization of the AgNPs, further emphasizing the eco-friendly and sustainable nature of the synthesis method.

The use of leaf extracts for nanoparticle synthesis offers numerous advantages over conventional chemical methods, including the avoidance of toxic chemicals and the feasibility of large-scale production. This research work contributes to the growing field of

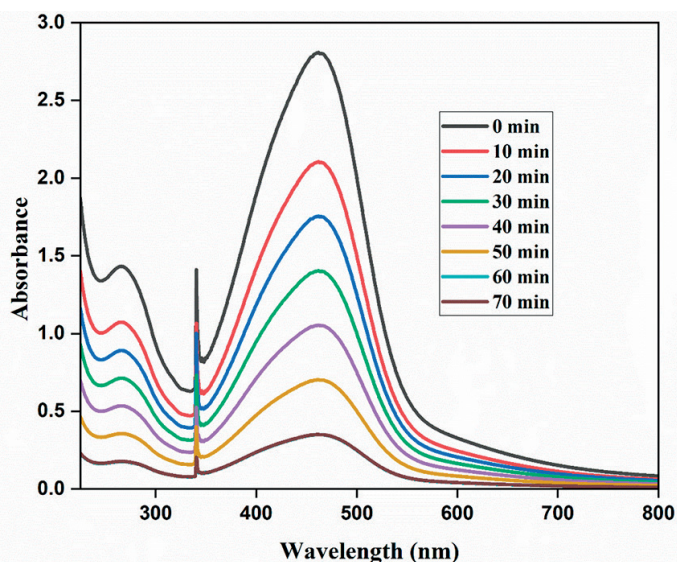
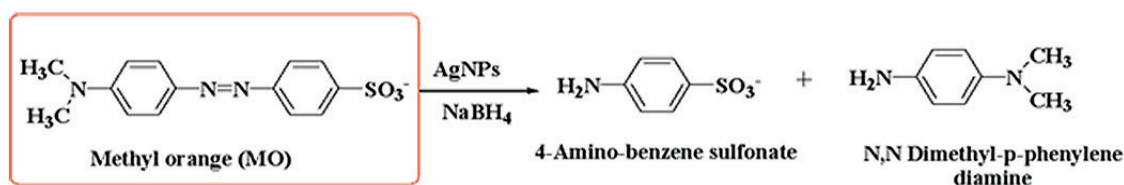


Figure 17: UV-vis. spectrum of catalytic reduction of methyl orange by NaBH_4 in the presence of AgNP-CA



Scheme 2: Degradation mechanism of methyl red and methyl orange

green nanotechnology by exploring the potential of *Coleus anthonyi* leaf extract as a natural source for the synthesis of metal nanoparticles. The findings of this study lay the foundation for future research endeavors, aiming to further explore the applications of AgNP-CA in various fields such as medicine, agriculture, and electronics. The eco-friendly synthesis route presented in this work serves as a promising alternative to conventional methods, offering sustainable solutions with reduced environmental impact. This research work not only highlights the potential of *Coleus anthonyi* as a valuable resource for green synthesis but also contributes to the broader understanding of plant-mediated nanoparticle synthesis and its implications in advancing sustainable technologies.

AUTHOR CONTRIBUTIONS

R Sunil: synthesis, formal analysis, investigation.

J Joseph: methodology, conceptualization.

T Sajini: supervision.

FUNDING

This research received no external funding.

CONFLICTS OF INTEREST

There are no conflicts to declare.

DATA AVAILABILITY STATEMENT

Data are available upon reasonable request.

ORCIDS

T Sajini: <https://orcid.org/0000-0002-1819-8153>

J Joseph: <https://orcid.org/0000-0002-2194-2529>

REFERENCES

1. Khan A, Ahmad N, Fazal H, Ali M, Akbar F, Khan I, Tayyab M, Uddin MN, Ahmad N, Abdel-Maksoud MA, et al. Biogenic synthesis of silver nanoparticles using *Rubus fruticosus* extract and their antibacterial efficacy against *Erwinia caratovora* and *Ralstonia solanacearum* phytopathogens. *RSC Adv.* 2024;14(9):5754–5763. <https://doi.org/10.1039/D3RA06723H>.
2. Raut S, Bhatavadekar A, Chougule R, Lekhak U. Silver nanoparticles synthesis from *Crinum moorei*: Optimization, characterization, kinetics and catalytic application. *S Afr J Bot.* 2024;165:494–504. <https://doi.org/10.1016/j.sajb.2024.01.005>.
3. Zhang Z, Shen W, Xue J, Liu Y, Liu Y, Yan P, Liu J, Tang J. Recent advances in synthetic methods and applications of silver nanostructures. *Nanoscale Res Lett.* 2018;13(1):54–66. <https://doi.org/10.1186/s11671-018-2450-4>.
4. Lee SH, Jun BH. Silver nanoparticles: synthesis and application for nanomedicine. *Int J Mol Sci.* 2019;20(4):865–867. <https://doi.org/10.3390/ijms20040865>.
5. Abou El-Nour KMM, Eftaiha A, Al-Warthan A, Ammar RAA. Synthesis and applications of silver nanoparticles. *Arab J Chem.* 2010;3(3):135–140. <https://doi.org/10.1016/j.arabj.2010.04.008>.
6. Kaur R, Mishra A, Saha S. An overview of phyto-assisted fabrication of metallic nanoparticles. *Biocatal Agric Biotechnol.* 2023;50:102723. <https://doi.org/10.1016/j.bcab.2023.102723>.
7. Shnawa BH, Mhammedsharif RM, Jalil PJ, Hamadamin SI, Ahmad SE, Abdulrahman KM, Ahmed MH. Antimicrobial activity of plant-extract-mediated synthesis of Silver-Zinc Oxide nanocomposites and their acaricidal efficacy on *Hyalomma marginatum* ticks. *Biocatal Agric Biotechnol.* 2023;51:102765. <https://doi.org/10.1016/j.bcab.2023.102765>.
8. Vidyasagar N, Patel RR, Singh SK, Singh M. Green synthesis of silver nanoparticles: methods, biological applications, delivery and toxicity. *Mater Adv.* 2023;4(8):1831–1849. <https://doi.org/10.1039/D2MA01105K>.
9. Tippyawat P, Phromviyo N, Boueroy P, Chompoosor A. Green synthesis of silver nanoparticles in aloe vera plant extract prepared by a hydrothermal method and their synergistic antibacterial activity. *PeerJ.* 2016;4:e2589. <https://doi.org/10.7717/peerj.2589>.
10. He Y, Wei F, Ma Z, Zhang H, Yang Q, Yao B, Huang Z, Li J, Zeng C, Zhang Q. Green synthesis of silver nanoparticles using seed extract of: *alpinia katsumadai*, and their antioxidant, cytotoxicity, and antibacterial activities. *RSC Adv.* 2017;7(63):39842–39851. <https://doi.org/10.1039/C7RA05286C>.
11. He Y, Li X, Zheng Y, Wang Z, Ma Z, Yang Q, Yao B, Zhao Y, Zhang H. A green approach for synthesizing silver nanoparticles, and their antibacterial and cytotoxic activities. *New J Chem.* 2018;42(4):2882–2888. <https://doi.org/10.1039/C7NJ04224H>.
12. Joseph J, Mathew J, George KV. *Coleus anthonyi* (Lamiaceae): a new species from South Western Ghats, India. *Species.* 2020;21:337–342.
13. Ahmed S, Saifullah, Ahmad M, Swami BL, Ikram S. Saifullah, Ahmad M, Swami BL, Ikram S. Green synthesis of silver nanoparticles using *Azadirachta indica* aqueous leaf extract. *J Radiat Res Appl Sci.* 2016;9(1):1–7. <https://doi.org/10.1016/j.jrras.2015.06.006>.
14. Joseph S, Mathew B. Microwave assisted facile green synthesis of silver and gold nanocatalysts using the leaf extract of *Aerva lanata*. *Spectrochim Acta A Mol Biomol Spectrosc.* 2015;136:1371–1379. <https://doi.org/10.1016/j.saa.2014.10.023>.
15. Ahmed S, Ahmad M, Swami BL, Ikram S. A review on plants extract mediated synthesis of silver nanoparticles for antimicrobial applications: A green expertise. *J Adv Res.* 2016;7(1):17–28. <https://doi.org/10.1016/j.jare.2015.02.007>.
16. Siddiqi KS, Husen A, Rao RAK. A review on biosynthesis of silver nanoparticles and their biocidal properties. *J Nanobiotechnology.* 2018;16(1):14. <https://doi.org/10.1186/s12951-018-0334-5>.
17. Keat CL, Aziz A, Eid AM, Elmarzugi NA. Biosynthesis of nanoparticles and silver nanoparticles. *Bioresour Bioprocess.* 2015;2(47):2.
18. Chaudhary J, Tailor G, Yadav M, Mehta C. Green route synthesis of metallic nanoparticles using various herbal extracts: A review. *Biocatal Agric Biotechnol.* 2023;50:102692. <https://doi.org/10.1016/j.bcab.2023.102692>.
19. Theertha KP, Tissamol A, Ashok SK, Revathy R, Sajini T. Exploring the antibacterial potential of green synthesized silver nanoparticle decorated on functionalized multi walled carbon nanotube : synthesis and analysis. *Chem Pap.* 2024;78(3):1601–1611. <https://doi.org/10.1007/s11696-023-03188-2>.
20. Okafor F, Janen A, Kukhtareva T, Edwards V, Curley M. Green synthesis of silver nanoparticles, their characterization, application and antibacterial activity. *Int J Environ Res Public Health.* 2013;10(10):5221–5238. <https://doi.org/10.3390/ijerph10105221>.
21. Chaudhary J, Tailor G, Mehta C, Yadav M. An overview of biosynthesized metallic nanoparticles via medicinal plant extracts of the Moraceae family. *Biocatal Agric Biotechnol.* 2023;52:102812. <https://doi.org/10.1016/j.bcab.2023.102812>.
22. Saha S, Malik MM, Qureshi MS. Microwave Synthesis of Silver Nanoparticles. *Nano Hybrids.* 2013;4:99–112. <https://doi.org/10.4028/www.scientific.net/NH.4.99>.
23. Seku K, Gangapuram BR, Pejaji B, Kadimpati KK, Golla N. Microwave-assisted synthesis of silver nanoparticles and their application in catalytic, antibacterial and antioxidant activities. *J Nanostructure Chem.* 2018;8(2):179–188. <https://doi.org/10.1007/s40097-018-0264-7>.
24. Vijayan R, Joseph S, Mathew B. Green synthesis of silver nanoparticles using *Nervalia zeylanica* leaf extract and evaluation of their antioxidant, catalytic, and antimicrobial potentials. *Particul Sci Technol.* 2019;37(7):809–815. <https://doi.org/10.1080/02726351.2018.1450312>.
25. Sreeram KJ, Nidhin M, Nair BU. Microwave assisted template synthesis of silver nanoparticles. *Bull Mater Sci.* 2008;31(7):937–942. <https://doi.org/10.1007/s12034-008-0149-3>.
26. Abou El-Nour KMM, Eftaiha A, Al-Warthan A, Ammar RAA. Synthesis and applications of silver nanoparticles. *Arab J Chem.* 2010;3(3):135–140. <https://doi.org/10.1016/j.arabj.2010.04.008>.
27. Murphy M, Ting K, Zhang X, Soo C, Zheng Z. Current Development of Silver Nanoparticle Preparation, Investigation, and Application in the Field of Medicine. *J Nanomater.* 2015;2015:696918. <https://doi.org/10.1155/2015/696918>.
28. Vidhu VK, Philip D. Catalytic degradation of organic dyes using biosynthesized silver nanoparticles. *Micron.* 2014;56:54–62. <https://doi.org/10.1016/j.micron.2013.10.006>.
29. Gudikandula K, Charya Maringanti S. Synthesis of silver nanoparticles by chemical and biological methods and their antimicrobial properties. *J Exp Nanosci.* 2016;11(9):714–721. <https://doi.org/10.1080/17458080.2016.1139196>.

30. Wei S, Wang Y, Tang Z, Hu J, Su R, Lin J, Zhou T, Guo H, Wang N, Xu R. A size-controlled green synthesis of silver nanoparticles by using the berry extract of Sea Buckthorn and their biological activities. *New J Chem.* 2020;44(22):9304–9312. <https://doi.org/10.1039/D0NJ01335H>.
31. Hemlata, Meena PR, Singh AP, Tejavath KK. Biosynthesis of silver nanoparticles using *Cucumis prophetarum* aqueous leaf extract and their antibacterial and antiproliferative activity against cancer cell lines. *ACS Omega.* 2020;5(10):5520–5528. <https://doi.org/10.1021/acsomega.0c00155>.
32. Shobana N, Prakash P, Samrot AV, Saigeetha S, Sathiyasree M, Thirugnanasambandam R, Sridevi V, Basanta Kumar M, Gokul Shankar S, Dhiva S, et al. Nanotoxicity studies of *Azadirachta indica* mediated silver nanoparticles against *Eudrilus eugeniae*, *Danio rerio* and its embryos. *Biocatal Agric Biotechnol.* 2023;47:102561. <https://doi.org/10.1016/j.bcab.2022.102561>.
33. Ramya R. GC-MS Analysis of Bioactive Compounds in Ethanolic Leaf Extract of *Hellenia speciosa* (J.Koenig) S.R. Dutta. *Appl Biochem Biotechnol.* 2022;194(1):176–186. <https://doi.org/10.1007/s12010-021-03742-2>.
34. Olivia NU, Goodness UC, Obinna OM. Phytochemical profiling and GC-MS analysis of aqueous methanol fraction of *Hibiscus asper* leaves. *Futur J Pharm Sci.* 2021;7:59. <https://doi.org/10.1186/s43094-021-00208-4>.
35. Konappa N, Udayashankar AC, Krishnamurthy S, Pradeep CK, Chowdappa S, Jogaiah S. GC-MS analysis of phytoconstituents from *Amomum nilgiriicum* and molecular docking interactions of bioactive serverogenin acetate with target proteins. *Sci Rep.* 2020;10(1):16438. <https://doi.org/10.1038/s41598-020-73442-0>.
36. Cartus AT, Stegmüller S, Simson N, Wahl A, Neef S, Kelm H, Schrenk D. Hepatic Metabolism of Carcinogenic β -Asarone. *Chem Res Toxicol.* 2015;28(9):1760–1773. <https://doi.org/10.1021/acs.chemrestox.5b00223>.
37. Venkatesan R, Karupiah PS, Arumugam G, Balamuthu K. β -Asarone Exhibits Antifungal Activity by Inhibiting Ergosterol Biosynthesis in *Aspergillus niger* ATCC 16888. *Proc Natl Acad Sci, India, Sect B Biol Sci.* 2019;89(1):173–184. <https://doi.org/10.1007/s40011-017-0930-4>.
38. Arironang HF, Koleangan H, Wuntu AD. Synthesis of silver nanoparticles using aqueous extract of medicinal plants' (*Impatiens balsamina* and *Lantana camara*) fresh leaves and analysis of antimicrobial activity. *Int J Microbiol.* 2019;2019:8642303. <https://doi.org/10.1155/2019/8642303>.
39. Pirtarighat S, Ghannadnia M, Baghshahi S. Green synthesis of silver nanoparticles using the plant extract of *Salvia spinosa* grown in vitro and their antibacterial activity assessment. *J Nanostructure Chem.* 2019;9(1):1–9. <https://doi.org/10.1007/s40097-018-0291-4>.
40. Singh D, Rawat D, Isha. Microwave-assisted synthesis of silver nanoparticles from *Origanum majorana* and *Citrus sinensis* leaf and their antibacterial activity: a green chemistry approach. *Bioresour Bioprocess.* 2016;3:14. <https://doi.org/10.1186/s40643-016-0090-z>.
41. Bhakya S, Muthukrishnan S, Sukumaran M, Muthukumar M. Biogenic synthesis of silver nanoparticles and their antioxidant and antibacterial activity. *Appl Nanosci.* 2016;6(5):755–766. <https://doi.org/10.1007/s13204-015-0473-z>.
42. Ibrahim HMM. Green synthesis and characterization of silver nanoparticles using banana peel extract and their antimicrobial activity against representative microorganisms. *J Radiat Res Appl Sci.* 2015;8(3):265–275. <https://doi.org/10.1016/j.jrras.2015.01.007>.
43. Sagar V, Patel RR, Singh SK, Singh M. Green synthesis of silver nanoparticles: methods, biological applications, delivery and toxicity. *Mater Adv.* 2023;8:1831–1849. <https://doi.org/10.1039/D2MA01105K>.
44. Talabani RF, Hamad SM, Barzinjy AA, Demir U. Biosynthesis of silver nanoparticles and their applications in harvesting sunlight for solar thermal generation. *Nanomaterials (Basel).* 2021;11(9):2421–2432. <https://doi.org/10.3390/nano11092421>.
45. Elumalai D, Hemavathi M, Deepaa CV, Kaleena PK. Evaluation of phytosynthesised silver nanoparticles from leaf extracts of *Leucas aspera* and *Hyptis suaveolens* and their larvicidal activity against malaria, dengue and filariasis vectors. *Parasite Epidemiol Control.* 2017;2(4):15–26. <https://doi.org/10.1016/j.parepi.2017.09.001>.
46. Mouriya GK, Mohammed M, Azmi AA, Khairul WM, Karunakaran T, Amirul AAA, Ramakrishna S, Santhanam R, Vigneswari S. Green synthesis of *Cicer arietinum* waste derived silver nanoparticle for antimicrobial and cytotoxicity properties. *Biocatal Agric Biotechnol.* 2023;47:102573. <https://doi.org/10.1016/j.bcab.2022.102573>.
47. Choudhary MK, Kataria J, Cameotra SS, Singh J. A facile biomimetic preparation of highly stabilized silver nanoparticles derived from seed extract of *Vigna radiata* and evaluation of their antibacterial activity. *Appl Nanosci.* 2016;6(1):105–111. <https://doi.org/10.1007/s13204-015-0418-6>.
48. Valdez-Salas B, Beltran-Partida E, Mendez-Trujillo V, González-Mendoza D. Silver nanoparticles from *Hpytus suaveolens* and their effect on biochemical and physiological parameter in mesquite plants. *Biocatal Agric Biotechnol.* 2020;28:101733. <https://doi.org/10.1016/j.bcab.2020.101733>.
49. Sambangi P, Gopalakrishnan S. Streptomyces-mediated synthesis of silver nanoparticles for enhanced growth, yield, and grain nutrients in chickpea. *Biocatal Agric Biotechnol.* 2023;47:102567. <https://doi.org/10.1016/j.bcab.2022.102567>.
50. Jyoti K, Baunthiyal M, Singh A. Characterization of silver nanoparticles synthesized using *Urtica dioica* Linn. leaves and their synergistic effects with antibiotics. *J Radiat Res Appl Sci.* 2016;9(3):217–227. <https://doi.org/10.1016/j.jrras.2015.10.002>.
51. Ashraf H, Anjum T, Riaz S, Naseem S. Microwave-Assisted Green Synthesis and Characterization of Silver Nanoparticles Using *Melia azedarach* for the Management of *Fusarium Wilt* in Tomato. *Front Microbiol.* 2020;11:238–257. <https://doi.org/10.3389/fmicb.2020.00238>.
52. Somasundaram CK, Atchudan R, Edison TNJI, Perumal S, Vinodh R, Sundramoorthy AK, Babu RS, Alagan M, Lee YR. Sustainable synthesis of silver nanoparticles using marine algae for catalytic degradation of methylene blue. *Catalysts.* 2021;11(11):1377–1389. <https://doi.org/10.3390/catal11111377>.
53. Ali IAM, Ahmed AB, Al-Ahmed HI. Green synthesis and characterization of silver nanoparticles for reducing the damage to sperm parameters in diabetic compared to metformin. *Sci Rep.* 2023;13(1):2256. <https://doi.org/10.1038/s41598-023-29412-3>.
54. Joseph S, Mathew B. Microwave-assisted facile synthesis of silver nanoparticles in aqueous medium and investigation of their catalytic and antibacterial activities. *J Mol Liq.* 2014;197:346–352. <https://doi.org/10.1016/j.molliq.2014.06.008>.
55. Bhanekar A, Giri M, Yadav K, Jaggi N. Study on degradation of methyl orange-an azo dye by silver nanoparticles using UV-Visible spectroscopy. *Indian J Phys Proc Indian Assoc Cultiv Sci.* 2014;88(11):1191–1196. <https://doi.org/10.1007/s12648-014-0555-x>.
56. Khodashenas B, Ghorbani HR. Synthesis of silver nanoparticles with different shapes. *Arab J Chem.* 2019;12(8):1823–1838. <https://doi.org/10.1016/j.arabjc.2014.12.014>.
57. Guilger-Casagrande M, de Lima R. Synthesis of Silver Nanoparticles Mediated by Fungi: A Review. *Front Bioeng Biotechnol.* 2019;7:287. <https://doi.org/10.3389/fbioe.2019.00287>.
58. Burduşel AC, Gherasim O, Grumezescu AM, Mogoantă L, Ficai A, Andronescu E. Biomedical applications of silver nanoparticles: an up-to-date overview. *Nanomaterials (Basel).* 2018;8(9):681–706. <https://doi.org/10.3390/nano8090681>.
59. Castillo-Henríquez L, Alfaro-Aguilar K, Ugalde-Álvarez J, Vega-Fernández L, Montes de Oca-Vásquez G, Vega-Baudrit JR. Green synthesis of gold and silver nanoparticles from plant extracts and their possible applications as antimicrobial agents in the agricultural area. *Nanomaterials (Basel).* 2020;10(9):1763. <https://doi.org/10.3390/nano10091763>.